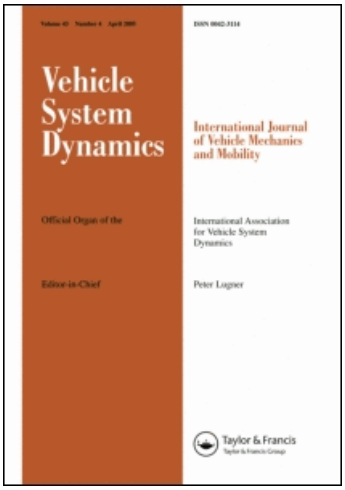

Vehicle System Dynamics

Publication details, including instructions for authors and subscription information:
http://www.informaworld.com/smpp/title~content=t713659010

Reference governors for controlled belt restraint systems

E. P. van der Laan [a]; W. P. M. H. Heemels [a]; H. Luijten [a]; F. E. Veldpaus [a]; M. Steinbuch [a]
[a] Department of Mechanical Engineering, Eindhoven University of Technology, Eindhoven, MB, The Netherlands

First published on: 23 October 2009

To cite this Article van der Laan, E. P., Heemels, W. P. M. H., Luijten, H., Veldpaus, F. E. and Steinbuch, M.(2009) 'Reference governors for controlled belt restraint systems', Vehicle System Dynamics,, First published on: 23 October 2009 (iFirst)
To link to this Article: DOI: 10.1080/00423110903154520
URL: http://dx.doi.org/10.1080/00423110903154520

Vehicle System Dynamics
2009, 1–20, iFirst

Taylor & Francis
Taylor & Francis Group

Reference governors for controlled belt restraint systems

E.P. van der Laan, W.P.M.H. Heemels, H. Luijten, F.E. Veldpaus and M. Steinbuch*

Department of Mechanical Engineering, Eindhoven University of Technology, PO Box 513, 5600 MB Eindhoven, The Netherlands

(*Received 20 February 2009; final version received 30 June 2009*)

Today's restraint systems typically include a number of airbags, and a three-point seat belt with load limiter and pretensioner. For the class of real-time controlled restraint systems, the restraint actuator settings are continuously manipulated during the crash. This paper presents a novel control strategy for these systems. The control strategy developed here is based on a combination of model predictive control and reference management, in which a non-linear device – a reference governor (RG) – is added to a primal closed-loop controlled system. This RG determines an optimal setpoint in terms of injury reduction and constraint satisfaction by solving a constrained optimisation problem. Prediction of the vehicle motion, required to predict future constraint violation, is included in the design and is based on past crash data, using linear regression techniques. Simulation results with MADYMO models show that, with ideal sensors and actuators, a significant reduction (45%) of the peak chest acceleration can be achieved, without prior knowledge of the crash. Furthermore, it is shown that the algorithms are sufficiently fast to be implemented online.

Keywords: passive safety; restraint systems; real-time control; reference governors; model predictive control; crash prediction

1. Introduction

Current restraint systems typically include a number of airbags and a three-point seat belt with load limiter and pretensioner [1]. These systems have to meet the safety regulations set by directive standards, for example from the US FMVSS [2] or the European Community. Within these regulations, the restraint configurations are geared to impact scenarios that are used in consumer tests, performed by crash rating agencies like USNCAP [3], IIHS [4], and EuroNCAP [5]. For frontal impacts, these scenarios involve standardised high-speed crashes (56, 64 kmph) against rigid or deformable offset barriers, with a 50th percentile adult male dummy. Additional testing is performed with the two extreme dummy types, viz., the 5th adult female and 95th male dummy.

The restraint configuration has usually one level of operation, and the level is chosen such that it gives as much protection as possible in the standardised crash tests. Although these

*Corresponding author. Email: m.steinbuch@tue.nl

ISSN 0042-3114 print/ISSN 1744-5159 online

DOI: 10.1080/00423110903154520
http://www.informaworld.com

tests are severe, the restraint design should be effective for a whole range of occupants and impact scenarios that can occur in reality. Without the possibility to optimise for the actual situation, the current design is a trade-off to maintain sufficient performance in all scenarios. This fundamental shortcoming of current restraint systems makes that not every vehicle occupant is optimally protected in every crash condition. To overcome this shortcoming, an increasing number of sensors and electronics is being integrated in vehicles. It allows the use of advanced restraint systems with adjustable components. These types of systems are called adaptive restraint systems, and its advancements over the past years will be discussed below.

1.1. *Adaptive Restraint Systems*

Occupant safety can be significantly improved by *adaptive* restraint systems. These restraint systems adjust their configuration during the crash according to the actual operating environment, such as occupant size, age or weight, occupant position, belt usage, and crash conditions. The flexibility of the restraint design allows to optimise the occupant's response for the actual situation. In literature, this type of restraint system has – confusingly – different names, like

smart [6–10], *intelligent* [11–13], *active* [14–17], or *adaptive* [18–21].

Many studies focus on *smart* adjustment of the tension in the safety belt to reduce thoracic injuries. The conventional load limiter that is part of most belt systems nowadays, enforces a constant load (4 or 6 kN) on the belt when activated. Studies have shown that an adjustable constant level in the belt restraint force improves thoracic injury mitigation, [8,10,22–24]. Dual-stage load limiters, which can switch once to a lower load level when desired, are able to lower the risk of thoracic injury even more, and examples can be found in [21,25]. Hence, advanced belt force manipulation may result in a significant lower injury risk to the thorax, especially for occupants or collisions that deviate from the average on which the regulations and tests are designed [18,25].

A near optimal protection can be delivered when the belt force can be continuously adapted during impact. In two similar studies [7,26] a time-varying belt force is applied in the open-loop. The optimal input is found through optimisation using an elementary chest model. More robust solutions are presented in [15–17,27,28], where the belt force is applied in a feedback configuration, and optimal values are obtained by solving a control problem. These types of systems, in which restraint settings can be continuously adapted during the crash, are referred to as *continuous restraint control* (CRC) systems.

The continuous manipulation of the restraint components, such as load limiter force, airbag vent size or belt roll-out, can be performed through a control algorithm. The objective of the controller is minimising one or more injury criteria (IC). Sensors provide information on restraint settings, biomechanical occupant responses, vehicle status, and motion. Based on these measurement data, the restraint actuator continuously alters the restraint components during the full duration of the crash. A schematic representation of the components of a CRC system is shown in Figure 1.

Although this class of restraint systems is not yet available in today's passenger vehicles, numerical simulations with a controlled seat belt and/or airbag show that a significant injury reduction can indeed be achieved [15,27,28]. Therefore, this class of systems will be a main focus of future restraint system development. This paper contributes to this development.

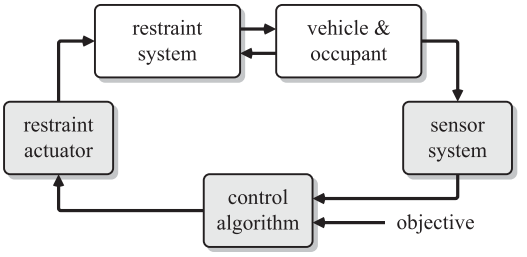

Figure 1. Schematic representation of a CRC system.

1.2. *Aim of this research*

In previous studies on controlled restraint systems, the control problem is formulated as a tracking problem, where biomechanical responses of the occupant are measured and forced to follow a reference trajectory. This trajectory results in a minimum risk of injury, while satisfying certain constraints. Through simulation studies, Hesseling *et al.* [27] showed promising results in terms of stability and tracking error, and significant reduction of IC. However, in [27], the reference trajectories are constructed assuming full *a priori* knowledge of the crash pulse, constraints, and occupant characteristics, which are clearly not realistic. The optimal trajectories heavily depend on the vehicle deceleration pulse during the crash, the occupant type and constraints such as the available space in the vehicle's interior. Moreover, optimisation strategies to derive optimal restraint settings as proposed in [7,15,26] are not likely to be solved in real-time, and still require knowledge of the vehicle motion during impact.

To harvest the advantages of using CRC systems, these limitations have to be overcome. This indicates the strong need for the development of a control algorithm that – based on the available measurements – computes the optimal control signals for the restraint actuator. The following requirements should be incorporated:

(i) the algorithm must be computationally feasible in order to meet the real-time requirements,
(ii) *a priori* knowledge of the crash pulse is not available, and
(iii) the algorithm must be based on online measurement data.

This paper proposes a solution to this challenging design problem. In particular, the study focuses on continuous control of the belt force, because – as discussed in Section 1.1 – this is very effective for thoracic injury mitigation.

1.3. *Contribution and outline*

The main contributions of this paper can be summarised as follows: (i) a control strategy is proposed that is able to determine optimal restraint settings *without a priori* crash information, aiming at a minimum risk of injury for the occupant, (ii) algorithms are developed, based on constrained optimisation problems, which implement the proposed control strategy and are able to run in real-time, (iii) simulation results with a force controlled seat belt and a MADYMO dummy model are presented that show a significant injury reduction for the thoracic region without pre-crash information.

The paper is organised as follows. Section 2 describes the approach to handle the constrained control and predictive problems at hand. The method consists of a setpoint optimisation and crash pulse prediction algorithm. These are explained in detail in Sections 3 and 4, respectively. Section 5 shows the simulation results. Finally, Section 6 provides the conclusions.

2. Control strategy

In this section, the control problem is mathematically formulated, and the adopted control strategy is presented.

2.1. *Formulation of the control problem*

As mentioned in the previous section, advanced belt loading may result in a significant lower injury risk to the thorax. Therefore, the control system aims at minimising the so-called thoracic IC, which are used in the field of impact biomechanics as indications for thoracic trauma. The following three ICs are widely accepted to assess thoracic trauma [29–31]:

(i) the peak chest acceleration, $A_{\max}$, is the maximum forward acceleration of the chest, $a_{\text{chest}}(t)$, that is maintained for 3 ms

$$A_{\max} := \max_t \left(\min_{\tau \in [0,3]\ \text{ms}} |a_{\text{chest}}(t+\tau)| \right) \tag{1}$$

(ii) the viscous criterion, VC, is the maximum value of the product of chest compression, $d(t)$, and its velocity of deformation, $\dot{d}(t)$,

$$\text{VC} := D \max_t \left(d(t)\dot{d}(t) \right) \tag{2}$$

with $D \geq 0$ a dummy or occupant-dependent constant scaling factor,

(iii) the peak chest compression, $D_{\max}$, is the maximum compression of the thorax

$$D_{\max} := \max_t d(t). \tag{3}$$

To determine these ICs, the biomechanical responses a_{chest}, d, and $\dot{d}$ are needed. These responses are generated by the system, P, consisting of the vehicle, the occupant and the restraint system, which are represented by the white blocks in Figure 1. The vehicle crash, denoted by signal w, is an exogenous disturbance input to P. As mentioned in Section 1.2, the available control input to influence this system, u, is the seat belt force, F_{belt}, that satisfies the following assumption:

ASSUMPTION 2.1 *The force in the seat belt, F_{belt}, can be continuously prescribed during an impact.*

Ongoing research in the field of belt restraint actuators makes it plausible that these actuators will be available in the near future, see, for example, the active damping device in [32].

The measured signals of system P are collected in the variable v and are available to the controller. Later on, these signals are exactly specified. The control scheme is sketched in Figure 2. An additional output x_{rel} is included, which is the chest displacement relative to the vehicle interior, i.e.

$$x_{\text{rel}}(t) := x_{\text{chest}}(t) - x_{\text{veh}}(t). \tag{4}$$

Here, x_{chest} is the chest position during impact, satisfying $a_{\text{chest}} = \ddot{x}_{\text{chest}}$. Furthermore, x_{veh} is the position of the B-pillar of the vehicle, that satisfies the following definition:

DEFINITION 2.2 *The moment of impact occurs at $t = 0$. The vehicle position is then defined to be zero, i.e. $x_{\text{veh}}(0) = 0$, and the vehicle velocity is given by $v_{\text{veh}}(0) = v_o$.*

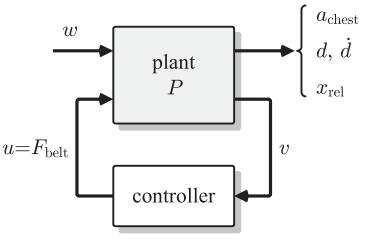

Figure 2. General control scheme, in which the seat belt force u is used to minimise thoracic IC of the system P, consisting of the vehicle, the occupant and the restraint system.

The output x_{rel} is relevant in the control problem. An upper-bound constraint on this output makes sure that the front seat occupant is not being too close to the steering wheel before the airbag deployment has been completed – causing even more severe injuries – and it prevents the rear seat occupant from hitting the front seat. A lower-bound constraint prevents the occupant from being pushed backwards through the seat. The constraints are given by

$$\bar{L}_1 \leq x_{\text{rel}}(t) \leq \bar{L}_2, \quad t \geq 0 \tag{5}$$

with $\bar{L}_1$ and $\bar{L}_2$ appropriate constants related to the position of the seat and steering wheel, respectively.

At this point, the focus lies on minimisation of the A_{max} criterion, but minimisation of the D_{max} or VC criteria can be added to this problem in a straightforward manner as well. As a consequence, the control problem at hand can be formulated as follows:

> Design a controller that prescribes the control input $u = F_{\text{belt}}$ to system P based on the information of the measurements v and given an (arbitrary) crash w, such that the criterium A_{max} in Equation (1) is minimised, while satisfying the constraint in Equation (5).

This constrained optimal control problem can be approached by model predictive control (MPC) or its ramifications.

2.2. *Model predictive control*

MPC, for example [33–37], is a widely used control technique that is able to handle control problems with input and state constraints. Typically, MPC utilises an explicit model of the to-be-controlled plant to predict the future output behaviour of the plant, on the basis of a measured or estimated current state and the chosen future input sequence. Its prediction capability allows to solve an optimal control problem over a finite future horizon, subject to constraints on state and input variables. MPC uses a receding horizon strategy in the sense that from the computed optimal input sequence, only the first control move is actually implemented. At the next sampling time, this optimisation problem is solved again on the basis of the updated state variables.

Solving the optimisation problem online is usually a time-consuming process, which is the reason that MPC in general requires a formidable computational effort. It is therefore mostly applied to slow or small processes, and clearly not during a vehicle crash.

More efficient methods to implement MPC algorithms have been considered recently. In explicit MPC [37–39], the optimisation problem is solved offline using multi-parametric programming. This results in a partitioning of the state space into different regions, and each region is associated with its own affine state feedback law. This might offer a solution to meet

the real-time requirements, if the determination of the correct region can be computed very fast. However, in many situations the number of regions is large, making the evaluation of the control function still demanding. At the current state of affairs, it is expected that explicit MPC will not be applicable to the complex system describing a vehicle occupant, and alternatives have to be considered.

2.2.1. *Reference governors*

Reference governors (RGs) reflect a predictive control method that acts on the setpoint or reference signal, rather than the control signal [40–43]. This has clear advantages from a computational and stability point of view. It can be seen as a subclass of MPC, and is sometimes referred to as reference management.

The RG acts on a system, in which the output y of plant P is already controlled by a feedback controller C. This system, consisting of P and C, is called the *primal controlled system*, G, and it is designed to track relevant references g with high accuracy. It is assumed that G is stable and has good tracking performance in spite of the presence of disturbances w, i.e. $y \approx g$. The main idea of reference management is to add an auxiliary non-linear device to the primal controlled system G (Figure 3). This device, the RG, determines r, a manipulable *virtual* reference. The virtual reference r would coincide with g when no constraints are present. In the case of input or state constraints on G, the RG modifies r whenever necessary to avoid (future) constraint violation. The RG uses the measurement v to determine constraint violation. This implies that an additional outer feedback loop is present. Bemporad has shown in [43] that stability of this outer loop – hence of the RG combined with the primal controlled system – is guaranteed for constant references, i.e. $\dot{g} = 0$. Hence, if the update period of the RG is considerably longer than the settling time of the closed-loop system, and under reasonable assumptions on g, stability of the combined system of RG and G as in Figure 3 can indeed be guaranteed.

RG forms an attractive alternative to MPC-like approaches, because of its computational efficiency. This makes RG of interest within the context of controlled restraint systems. For these reasons, the proposed control strategy will be based on RG as a subclass of MPC. In the following paragraph, it is explained how the RG method is tailored to solve the specific control problems outlined in Section 1.2.

2.3. *The approach*

The RG control strategy is particularly appealing, because of its computational efficiency and the separation of stability and performance. In literature, however, applications are limited to systems with constant reference signals or small disturbances. Since the optimal setpoint for

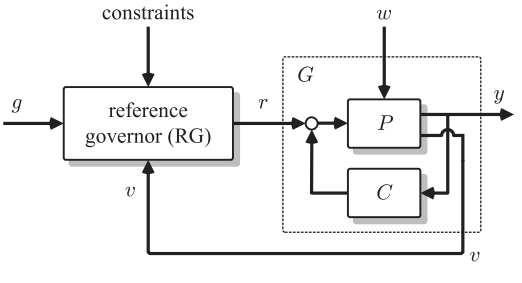

Figure 3. The RG approach.

the primal controlled system is not a constant, it is necessary to adapt the currently available methods for RG. Instead of modifying a desired reference, the virtual reference r is found by solving an optimisation problem online.

2.3.1. *The primal controlled system*

Following the control problem formulated in Section 2.1, the setpoint r should be constructed such that A_{max} is minimised, i.e. the 3 ms maximum of $|a_{chest}|$ as in Equation (1), subject to the dynamics of plant P and the inequality constraints in Equation (5). Now consider the following assumption:

ASSUMPTION 2.3 *An accurate estimate of the forward chest acceleration, a_{chest}, is available during the impact.*

This assumption is plausible, given the results presented in [44], where Kalman filters are used to estimate the chest acceleration from belt roll-out measurements. The output available for feedback is now taken $y = a_{chest}$, and a local feedback controller C, as already discussed in Section 2.2.1, is designed that aims at minimising $e = r - a_{chest}$ (Figure 4). Now the following is proposed with respect to the local controller:

ASSUMPTION 2.4 *A local feedback controller C can be designed such that the primal controlled system G, consisting of plant P and controller C, has ideal tracking performance, i.e. $a_{chest} = r$.*

This assumption can also be realised closely, as simulation results with complex and accurate occupant models indeed show excellent tracking behaviour, see, for example, [27,28].

2.3.2. *Two-step procedure*

With Assumptions 2.1 and 2.4 assumed to hold, finding the optimal signal r in terms of a minimal A_{max} does not require a model of the primal controlled system G, as $a_{chest} = r$. This allows to split the RG in two steps, being a *setpoint optimisation*, and a *crash prediction*. The first step is formulated as follows:

(1) *The setpoint optimisation*. Based on information on the internal state of the primal controlled system and a prediction of the future vehicle motion, determine a reference signal r that minimises one or more IC (here A_{max}) and satisfies the constraints in Equation (5).

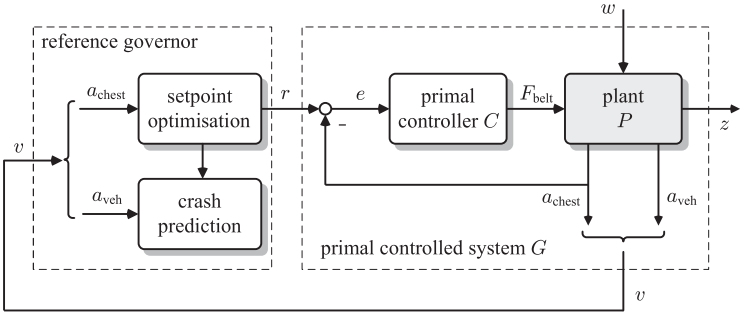

Figure 4. Adapted RG design with crash prediction for the primal controlled system.

In this step, a vehicle motion prediction is required. Since acceleration sensors are present in most consumer cars to detect a crash, the following assumption is plausible.

ASSUMPTION 2.5 *The vehicle acceleration pulse, a_{veh}, is available as a measurable signal during impact.*

Using this assumption, the second step of the RG can be formulated:

2. *The crash prediction*. Based on the entire history of the measured vehicle acceleration, predict the future vehicle motion.

Combining both steps leads to the overall RG design as shown in Figure 4. The RG is implemented in discrete time, and is executed every T_o seconds. Since this scheme typically results in better behaviour when executed more often during the crash, it must be computationally extremely efficient, especially given the short duration of the crash. In the next section, the setpoint optimisation step is presented in detail, while the crash prediction step follows in Section 4.

3. Setpoint optimisation

It is shown here that the setpoint optimisation problem can be written as a linear program (LP), which can be solved efficiently in limited time [45].

3.1. *The finite horizon*

The setpoint optimisation step solves a constrained optimisation problem using a prediction of the vehicle motion. To make this problem feasible in real-time, a finite prediction horizon is introduced in the constraint equation by using the following assumptions.

ASSUMPTION 3.1 *At $t = T_e$, the vehicle has come to a full stop, i.e., the velocity of the vehicle satisfies $v_{\text{veh}}(t) = 0$ for $t \geq T_e$.*

With crash data being widely available, a value T_e can easily be chosen such that this assumption is typically satisfied.

ASSUMPTION 3.2 *At $t = T_e$, the occupant has come close to a stop in the sense that the relative occupant velocity is within bounds $S_1 < 0 < S_2$, i.e.*

$$S_1 \leq v_{\text{rel}}(T_e) \leq S_2, \quad v_{\text{rel}}(t) = \dot{x}_{\text{rel}}(t) \tag{6}$$

with x_{rel} as in Equation (4).

Assumption 3.1 implies that the vehicle has no kinetic energy after time T_e. Given that the restraint systems only dissipate energy, the occupant's kinetic energy typically decreases to zero after time T_e. Hence, if Equation (6) is imposed for S_1 and S_2 sufficiently close to zero, and if

$$L_1 \leq x_{\text{rel}}(t) \leq L_2, \quad 0 \leq t \leq T_e \tag{7}$$

is imposed for a suitably chosen $L_1 > \bar{L}_1$ and $L_2 < \bar{L}_2$, then it is reasonable to assume that Equation (5) is satisfied. Hence, when the above assumptions hold, the infinite horizon in Equation (5) can be replaced by the finite horizon constraints in Equations (6) and (7).

The RG is executed every $T_o = T_e/N_1$ seconds on the interval $[0, T_e]$, with $N_1 \in \mathbb{N}$, where $\mathbb{N}$ is the set of positive integers. The measurable variables v are sampled on $[0, T_e]$ with sample time $T = T_o/N_2$, $N_2 \in \mathbb{N}$. Define $N_e := N_1 N_2$. The measurable variables are then available at time instances $t = kT$, with $k \in \mathbb{K} := \{0, 1, 2, \ldots, N_e\}$, and the RG is executed at time instances $t = kT$, with $k \in \mathbb{K}_o := \{0, N_2, 2N_2, \ldots, N_e\} \subseteq \mathbb{K}$. Furthermore, $n(k) := N_e - k$, which are the remaining number of samples in the interval $[kT, T_e]$. See Figure 5 for a graphical depiction of the time line.

For clarity of notation, the variables in discrete time are denoted by, for example, $v[k] = v(kT)$.

3.2. *Optimisation problem*

The optimisation problem from Section 2.1 can now be formulated mathematically. First, a relaxation is applied to the minimisation of the $A_{\max}$ criterion in Equation (1), based on

$$A_{\max} \leq \max_t |a_{\text{chest}}(t)| \,.$$

The right-hand part in this relation is an upper bound of the $A_{\max}$ criterion. There are clear advantages to use the upper bound in the optimisation problem instead of $A_{\max}$. First, the implementation is much more efficient from a numerical point of view, as only half of the optimisation variables are needed. Second, it will typically lead to an optimal solution where one sample of a_{chest} in the 3 ms interval is zero, whereas the remaining samples have very high values. This solution minimises $A_{\max}$, but is clearly undesirable and not implementable in practice.

With this relaxation, and supposing that Assumptions 2.1, 2.3, and 2.4 hold, the optimal control problem formulation with constraint Equations (6) and (7) is given in discrete time for $k \in \mathbb{K}_o$ by

$$\begin{array}{lll} \min\limits_{r} & \max\limits_{j\in\{0,\ldots,n(k)\}} |r[k+j]| & \\ \text{subject to} & L_1 \leq x_{\text{rel}}[k+j|k] \leq L_2, & j \in \{0,\ldots,n(k)\}. \\ & S_1 \leq v_{\text{rel}}[N_e|k] \leq S_2 & \end{array} \tag{8}$$

The notation $x_{\text{rel}}[\ell|k]$, with $\ell \in \mathbb{K}$, $\ell \geq k$, is used to denote the prediction of signal $x_{\text{rel}}[\ell]$ with knowledge up to time kT. Hence, at every optimisation instant $k \in \mathbb{K}_o$, the setpoint sequence r is chosen to minimise the maximal $r = a_{\text{chest}}$, while satisfying constraints on the relative displacement and on the final relative velocity.

3.2.1. *Prediction of absolute chest motion*

To solve this problem, the relative motions x_{rel} and v_{rel} have to be predicted on the basis of available information. It is chosen here to use a prediction model for the *absolute* chest motion,

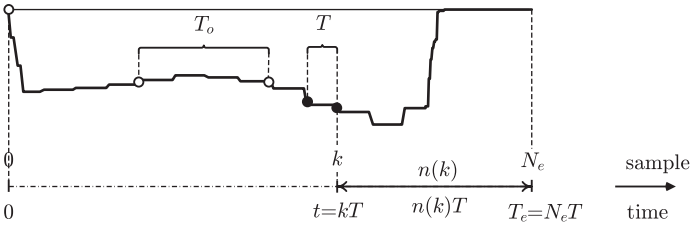

Figure 5. Time line of the signals. Measurements are available at discrete time instants $t = kT$ (•), with $k \in \mathbb{K}$. The RG is executed every T_o seconds, that is at times $t = kT$ (∘), with $k \in \mathbb{K}_o$. The length of the signals is $T_e = N_e T$.

instead of the relative chest motion. This is an important choice, as will become clear in the next section. The adopted prediction model is based on a simple first-order Euler integration scheme applied to $\ddot{x}_{\text{chest}} = a_{\text{chest}} = r$. This leads to the discrete-time model

$$\begin{aligned} x_{\text{chest}}[k+1|k] &= x_{\text{chest}}[k] + T v_{\text{chest}}[k] \\ v_{\text{chest}}[k+1|k] &= v_{\text{chest}}[k] + T r[k] \end{aligned} \tag{9}$$

in which Assumption 2.4 is used. When this model is executed recursively, the prediction of the relative motion can be written as

$$\begin{aligned} x_{\text{rel}}[\ell|k] &= x_{\text{chest}}[k] + (\ell - k) T v_{\text{chest}}[k] + T^2 \sum_{i=k+1}^{\ell-1} (\ell - i) r[i] - x_{\text{veh}}[\ell|k] \\ v_{\text{rel}}[N_e|k] &= v_{\text{chest}}[k] + T \sum_{i=k}^{N_e-1} r[i] - \underbrace{v_{\text{veh}}[N_e|k]}_{0} \end{aligned} \tag{10}$$

with $k \in \mathbb{K}$, $\ell \in \{k, \ldots, N_e\}$. In the second equation, Assumption 2.5 is used to set the predicted final vehicle velocity to zero.

The current states of the model in this equation, $x_{\text{chest}}[k]$ and $v_{\text{chest}}[k]$ are given by an 'open-loop observer', which is also based on a first Euler integration scheme applied to $\ddot{x}_{\text{chest}} = a_{\text{chest}}$:

$$\begin{aligned} x_{\text{chest}}[k] &= x_{\text{chest}}[0] + kT v_{\text{chest}}[0] + T^2 \sum_{i=0}^{k-1} (k - i) a_{\text{chest}}[i] \\ v_{\text{chest}}[k] &= v_{\text{chest}}[0] + T \sum_{i=0}^{k-1} a_{\text{chest}}[i] \end{aligned} \tag{11}$$

with $k \in \mathbb{K}$.

ASSUMPTION 3.3 *The initial relative chest position and velocity are assumed to be zero, hence with Definition* 2.2, $x_{\text{chest}}[0] = 0$ *and* $v_{\text{chest}}[0] = v_o$.

The observer model (11) can be plugged into the prediction model (10) to obtain

$$\begin{aligned} x_{\text{rel}}[\ell|k] &= T^2 \left(\sum_{i=0}^{k-1} (\ell - i) a_{\text{chest}}[i] + \sum_{i=k+1}^{\ell} (\ell - i) r[i] \right) + \ell T v_o - x_{\text{veh}}[\ell|k] \\ v_{\text{rel}}[N_e|k] &= v_o + T \left(\sum_{i=0}^{k-1} a_{\text{chest}}[i] + \sum_{i=k}^{N_e-1} r[i] \right) \end{aligned} \tag{12}$$

with $k \in \mathbb{K}$, $\ell \in \{k, \ldots, N_e\}$. Note that the constraint equations now depend on v_0, on the measurement history $a_{\text{chest}}[i]$ for $i = 0, \ldots, k-1$, on the future vehicle displacement prediction $x_{\text{veh}}[k + j|k]$ and on the virtual setpoint sequence $r[k + j]$ for $j = 0, \ldots, N_e - k$.

3.3. *Linear programming*

The min–max objective in Equation (8) can be rewritten as a LP by introducing an auxiliary variable $\gamma \geq 0$. This γ represents the maximum of the absolute value of $r(k + j)$.

Hence, Equation (8) becomes for $k \in \mathbb{K}_o$

$$\begin{array}{lccccc} \min\limits_{\mathbf{p}} & & & \gamma & & \\ \text{subject to} & -\gamma & \leq & r[k+j] & \leq & \gamma \quad j \in \{0, \ldots, n(k)\} \\ & L_1 & \leq & x_{\text{rel}}[k+j|k] & \leq & L_2 \\ & S_1 & \leq & v_{\text{rel}}[N_e|k] & \leq & S_2 \end{array} \tag{13}$$

where $\mathbf{p} \in \mathbb{R}^{n(k)+2}$ contains the input, i.e. the degrees of freedom, given by

$$\mathbf{p} = [r[k]\ r[k+1]\ \cdots\ r[N_e]\ \gamma]^{\mathrm{T}}.$$

When the above constraint equations are written in a matrix form using Equation (12), it is clear that the constraints also depend linearly on the optimisation vector $\mathbf{p}$. Then Equation (13) can be formulated as an LP

$$\begin{array}{ll} \min\limits_{\mathbf{p}} & \phi^{\mathrm{T}}\mathbf{p} \\ \text{subject to} & A_{\mathrm{p}}\mathbf{p} \leq \mathbf{b}_{\mathrm{p}} \end{array} \tag{14}$$

with $\phi = [0\ \ldots\ 0\ 1]^{\mathrm{T}} \in \mathbb{R}^{n(k)+2}$, and A_{p} and $\mathbf{b}_{\mathrm{p}}$ suitable vectors according to the constraint equations. The problem in Equation (14) can now be efficiently and accurately solved by simplex or interior point methods [45].

3.4. *Results*

The algorithm is implemented in Matlab/Simulink, and results are generated for $L_1 = -0.03$ m, $L_2 = 0.25$ m, $S_1 = -1$ m/s, $S_2 = 0$ m/s, $T = 0.1$ ms, $T_o = 10$ ms, and $T_e = 200$ ms. At this point, it is assumed that full *a priori* crash information on x_{veh} is available. Later, this information will come from the second step in the RG, namely the crash prediction step as shown in Figure 4.

Since the computational complexity of the problem (14) depends directly on the degrees of freedom in $\mathbf{p}$, a tractable optimisation problem can be obtained by fixing the inputs to be constant over a certain number of samples. This is known as the move blocking, see for example, [46]. In Equation (14), the number of inputs is reduced to 11, and the problem of finding the optimal $\mathbf{p}$ is restated as finding the optimal $\hat{\mathbf{p}}$, where $\mathbf{p} = M\hat{\mathbf{p}}$ and $M \in \mathbb{R}^{n(k)+2\times 11}$ is the so-called blocking matrix. M is assumed to be a matrix of ones and zeros only, with each row containing exactly one non-zero element. Correspondingly, constraint violation is checked at only 10 points on the future horizon. These two relaxations save valuable computational time, while they still lead to good performance, as will be shown later on.

Figure 6 shows the outcome of the simulation for a crash pulse obtained from a 40% offset frontal impact with a small family car against a deformable barrier at 64 km/h. The top left figure shows the pulse a_{veh} (grey) and the optimal setpoint r (black). One can see that a near optimal solution is found, in spite of the two relaxations described above.

At every time instant kT, $k \in \mathbb{K}_o$, the optimal solution was found within 6 ms – see figure on the top right – on an average workstation[1], which is below the available time of $T_o = 10$ ms. Of course, with dedicated algorithms and hardware, this can easily be improved further. The decrease in calculation times is caused by the fact that blocking matrix M decreases in size, as the future horizon length decreases, although the number of inputs remains constant. The bottom two figures show that the constraints are not violated.

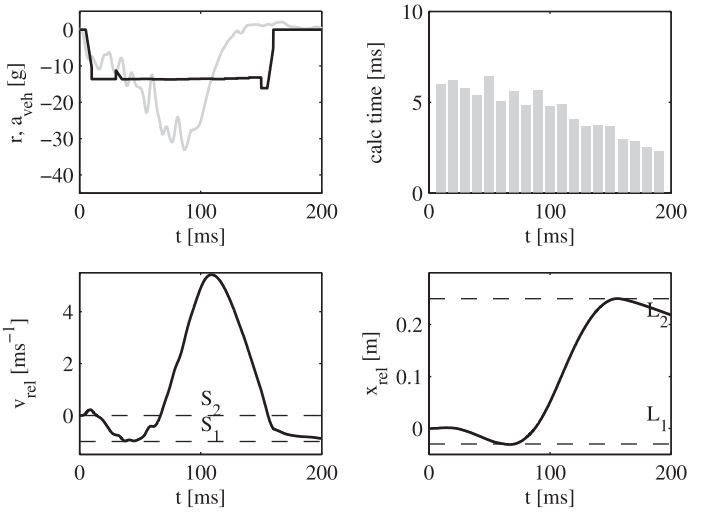

Figure 6. *Top*: Left: The optimal setpoint (solid) for the chest acceleration given a vehicle acceleration (dash-dotted). Right: Calculation times at every optimisation step T_o. Bottom: The relative chest displacement does not violate the constraints.

3.5. *Conclusion*

In this section, the setpoint optimisation step has been developed that generates a setpoint for the primal controlled system shown in Figure 4. This setpoint is optimal in a sense that an upper bound on the $A_{\max}$ criteria is minimised while satisfying the constraint in Equation (5). It was shown that a finite prediction horizon suffices when this constraint is replaced by Equations (6) and (7). Using the models (10) and (11), the optimisation problem could be written as an LP. To solve this LP, we need to know the initial vehicle velocity, a measurement of the current chest acceleration and a prediction of the future vehicle displacement. With assumed *a priori* knowledge of the latter, the obtained setpoint for a given crash pulse was shown to be near optimal, and it was found within milliseconds due to a move blocking procedure.

4. Prediction of vehicle motion

Knowledge of the future vehicle motion is obviously not available during the crash. In this section, an algorithm is presented to predict this motion.

The algorithm presented in the previous section has a very important advantage. From Equation (10), it became clear that the future vehicle displacement $x_{\text{veh}}(k+j|k)$, for $j = 1, \ldots, n(k)$, should be known. Note that if the prediction model in Equation (9) would have been applied to x_{rel} instead of x_{chest}, which is more intuitive as the constraints are imposed on x_{rel}, a prediction of the crash pulse a_{veh} would have been required instead of the crash displacement x_{veh}. This is an important advantage, as the displacement is a far smoother signal than the acceleration and can therefore be much better estimated.

4.1. *Objective function*

It is proposed to fit a vehicle displacement function, $f_x : \mathbb{R} \to \mathbb{R}$, to the history of x_{veh} by regression analysis. This function $f_x(t)$ is chosen to be twice differentiable in t, such that

$\dot{f}_x$ and $\ddot{f}_x$ are the vehicle velocity and acceleration functions, respectively. The optimal fit is found by minimisation of an objective function, J. The optimal vehicle displacement function, f_x, is used to predict the future vehicle displacement as follows:

$$x_{\text{veh}}[k+j|k] = f_{\text{x}}((k+j)T), \quad j = 1, \ldots, n(k) \tag{15}$$

for $k \in \mathbb{K}_o$.

The objective function, J, consists of the sum of the squared error between the measured past displacement and the function evaluations f_x. The squared error between measured current velocity and acceleration, and the velocity and acceleration function are both included in J as well. Previously, it was assumed that the vehicle will reach zero velocity at time T_e (Assumption 3.1). Therefore, it is required that the vehicle has zero velocity at an *additional* 10 time instant after T_e with a time separation of $\tau = 5\,\text{ms}$. This objective forms the last part of J. Hence, the objective function J for $k \in \mathbb{K}_o$ reads

$$\begin{aligned} J[k] = \sum_{j=0}^{k} & |f_{\text{x}}(jT) - x_{\text{veh}}[j]|^2 + \\ & \beta_1^2 |\dot{f}_{\text{x}}(kT) - v_{\text{veh}}[k]|^2 + \\ & \beta_2^2 |\ddot{f}_{\text{x}}(kT) - a_{\text{veh}}[k]|^2 \\ & \beta_3^2 \sum_{j=0}^{10} |\dot{f}_{\text{x}}(T_e + j\tau) - 0|^2 + \end{aligned} \tag{16}$$

where $\beta_i > 0, i = 1, 2, 3$ are weighting constants. The objective function (16) requires knowledge of the current values of v_{veh} and a_{veh}, and the history of x_{veh}. According to Assumption 2.5, only the vehicle acceleration is available for measurement. Therefore, again an 'open-loop observer' is used similar to Equation (11), hence:

$$\begin{aligned} x_{\text{veh}}[k] &= 0 + kTv_o + T^2 \sum_{i=0}^{k-1} (k-i) a_{\text{veh}}[i] \\ v_{\text{veh}}[k] &= v_o + T \sum_{i=0}^{k-1} a_{\text{veh}}[i]. \end{aligned} \tag{17}$$

In these equations, knowledge of the initial vehicle velocity is required. Now consider the following:

ASSUMPTION 4.1 *The vehicle speed at the moment of impact, v_0, is known.*

This is a reasonable assumption, since the vehicle's speedometer can be used to determine the speed just before impact. Note that this is a good estimate when there is low slip, which is often the case as anti-locking brake systems are available in most consumer vehicles.

The objective J now only depends on the measured vehicle acceleration a_{veh}, and the known initial speed v_0.

4.2. *Linear regression*

To solve the minimisation of J, a polynomial structure of order m is imposed on f_x:

$$f_x(t) = q_0 + q_1 t + q_2 t^2 + q_3 t^3 + \cdots + q_m t^m$$

with $q_i \in \mathbb{R}, i = 0, \ldots, m$. It follows from Definition 2.2 that $q_0 = 0$ and $q_1 = v_o$. The remaining parameters are stacked in a parameter vector $\mathbf{q} = [q_2\ q_3\ \cdots\ q_m]^{\mathrm{T}}$. The vehicle motion functions can be written linearly in $\mathbf{q}$, as follows:

$$\begin{aligned} f_x(t) &= \psi_x(t)\mathbf{q} + v_o t \\ \dot{f}_x(t) &= \dot{\psi}_x(t)\mathbf{q} + v_o \\ \ddot{f}_x(t) &= \ddot{\psi}_x(t)\mathbf{q} \end{aligned} \tag{18}$$

with vector function $\boldsymbol{\psi}_x : \mathbb{R} \to \mathbb{R}^{m-1}$ given by

$$\boldsymbol{\psi}_x(t) = [t^2\ t^3\ \cdots\ t^m].$$

When Equations (18) and (17) are substituted into Equation (16), the minimisation of the objective function can be rewritten as

$$\min_{\mathbf{q}} \left\| A_q \mathbf{q} - \mathbf{b}_{\mathrm{q}} \right\|_2^2 \tag{19}$$

with matrices A_q and $\mathbf{b}_q$ as follows

$$A_{\mathrm{q}} = \begin{bmatrix} \psi_x(T) \\ \psi_x(2T) \\ \psi_x(3T) \\ \vdots \\ \psi_x(kT) \\ \hline \beta_1 \cdot \dot{\psi}_x(kT) \\ \beta_2 \cdot \ddot{\psi}_x(kT) \\ \hline \beta_3 \cdot \dot{\psi}_x(T_e) \\ \beta_3 \cdot \dot{\psi}_x(T_e + \tau) \\ \vdots \\ \beta_3 \cdot \dot{\psi}_x(T_e + 10\tau) \end{bmatrix}, \quad \mathbf{b}_{\mathrm{q}} = \begin{bmatrix} 0 & 0 & 0 & \cdots & 0 & 0 \\ 0 & T^2 & 0 & \cdots & 0 & 0 \\ 0 & 2T^2 & T^2 & \cdots & 0 & 0 \\ \vdots & \vdots & \vdots & \ddots & \vdots & \vdots \\ 0 & (k-1)T^2 & (k-2)T^2 & \cdots & T^2 & 0 \\ \hline 0 & \beta_1 T & \beta_1 T & \cdots & \beta_1 T & 0 \\ 0 & 0 & 0 & \cdots & 0 & \beta_2 \\ \hline -\beta_3 & 0 & 0 & \cdots & 0 & 0 \\ -\beta_3 & 0 & 0 & \cdots & 0 & 0 \\ \vdots & \vdots & \vdots & \ddots & \vdots & \vdots \\ -\beta_3 & 0 & 0 & \cdots & 0 & 0 \end{bmatrix} \times \begin{bmatrix} v_0 \\ a_{\mathrm{veh}}(0) \\ a_{\mathrm{veh}}(1) \\ \vdots \\ a_{\mathrm{veh}}(k) \end{bmatrix}.$$

It is well-known, see, for example, [45], that the analytical solution to the linear regression problem in Equation (19) is $\mathbf{q}^* = (A_q^T A_q)^{-1} A_q^T \mathbf{b}_q$, assuming A_q has full column rank. Since the top block of A_q has linearly independent columns and has dimensions $k \times (m-1)$, one can easily verify that A_q has full column rank for all $k \geq m - 1$. So the optimal solution exists, when there are at least as many data points available as the order of the polynomial function f_x. Or in other words, the vehicle prediction can successfully be executed for the first time at $t = mT$.

With the optimal solution $\mathbf{q}^*$ and Equations (18) and (15), the prediction for x_{veh} reads for $k \in \mathbb{K}_o$ as follows:

$$x_{\mathrm{veh}}[k + j|k] = \psi_x((k + j)T)\mathbf{q}^* + (k + j)T v_0, \quad j \in \{1, \ldots, n(k)\}.$$

The vehicle prediction is now used in the prediction model of the relative chest displacement, see Equation (12), and it only depends on measurements of a_{veh} and v_0.

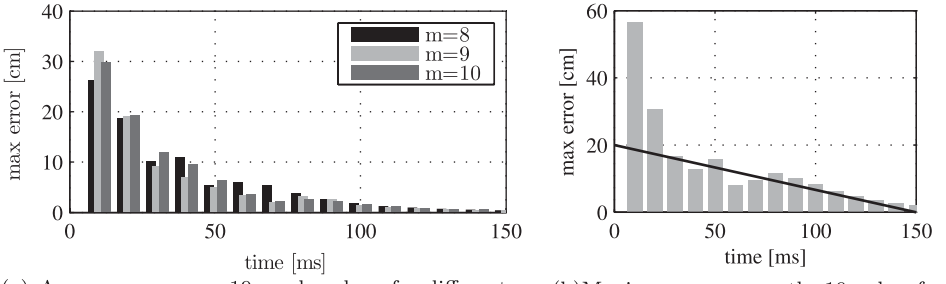

(a) Average error over 19 crash pulses, for different approximation orders m.

(b)Maximum error over the 19 pulses for m= 9, with robustness function ϵ_x.

Figure 7. Prediction error values for 19 frontal crash pulses, according to the error criterium in Equation (20).

4.3. *Results*

A large set of crash pulses, obtained from data from frontal EuroNCAP and USNCAP impact tests, is used to evaluate the accuracy of the algorithm. The absolute error between the predicted displacement and the actual future vehicle displacement is calculated at every optimisation step T_o. So for $k \in \mathbb{K}_o$

$$e[k] = \max_{j \in \{1,\ldots,n(k)\}} |f_{\mathrm{x}}((k+j)T) - x_{\mathrm{veh}}[k+j]| \,. \tag{20}$$

These error values are determined for 19 different crash pulses, and then averaged. Figure 7(a) shows the error values $e(k)$, $k \in \mathbb{K}_o$ for three different approximation orders $m = 8, 9, 10$, and for $T_o = 10\,\mathrm{ms}$, $T = 0.1\,\mathrm{ms}$, $\beta_1 = \beta_2 = 1$, $\beta_3 = 10$, and $T_e = 0.2\,\mathrm{s}$. The prediction algorithm is first executed at time $t = T_o$, so then $k = T_o/T = 100 \gg m$ and the optimal solution exists.

The results show that for $m = 9$, the best results are obtained, leading to errors of less than 10 cm after 30 ms. Similar tests have been performed to obtain the optimal values of β_i, $i = 1, 2, 3$. Given that the desired relative displacement of the chest is in the order of 25 cm, the obtained error values are acceptable. Especially since the setpoint optimisation can adapt online to mismatches, as will also be shown in Section 5, where the setpoint optimisation and crash prediction are combined. So, although the crashes differ substantially in magnitude, impact velocity and duration, the displacement is predicted with reasonable accuracy.

5. Simulation results with the adapted RG

In this section, the results are shown for the complete RG, which combines the setpoint optimisation and the vehicle prediction, as depicted in Figure 4. To accommodate the prediction errors of the future vehicle displacement path, see Figure 7(b) a robustified version of the setpoint optimisation algorithm is proposed first.

5.1. *Robustness*

The information about the maximum prediction error at every time instant k is shown in Figure 7(b). It is used in the setpoint optimisation problem to cope with the uncertainty in the prediction. This will be done using the so-called robustness function $\epsilon_x : \mathbb{R} \to \mathbb{R}$. It is a function of time, and it is assumed that the maximum absolute error in the prediction of x_{veh}

will be less than this function, in the sense that

$$\max_{j\in\{1,\ldots,n(k)\}} |x_{\text{veh}}[k+j|k] - x_{\text{veh}}[k+j]| \leq \epsilon_x[k], \quad k \in \mathbb{K}_o. \tag{21}$$

The function $\epsilon_x(t)$ decreases over time, as the maximum prediction error over 19 pulses also decreases, as can be seen in Figure 7(b). The function is chosen as

$$\epsilon_x(t) = \begin{cases} 0.20 - 1.33\,t & \text{for } t \leq 0.15 \\ 0 & \text{for } 0.15 < t \end{cases}$$

and is indicated in Figure 7(b) by the black line. In this function, ϵ_x is given in meters, and t in seconds. The setpoint optimisation algorithm is made robust against this inevitable vehicle prediction error. The robustified version of the optimisation problem is obtained by decreasing the constraints with $\epsilon_x[k]$. So for $k \in \mathbb{K}_o$

$$\begin{aligned} \min_{r} \quad & \max_{j\in\{1,\ldots,n(k)\}} |r[k+j]| \\ \text{subject to} \quad & L_1 + \epsilon_x[k] \leq x_{\text{rel}}[k+j|k] \leq L_2 - \epsilon_x[k] \\ & S_1 \leq v_{\text{rel}}[N_e|k] \leq S_2. \end{aligned} \tag{22}$$

Clearly, the constraint on x_{rel} in this optimisation problem together with the relationship (21), guarantees that $L_1 \leq x_{\text{rel}}[k+j|k] \leq L_2$ as in the original problem. Besides, since ϵ_x is a decreasing function, the bounds become less conservative as the crash progresses and more information becomes available. Towards the end of the crash, the original constraint as in Equation (8) is recovered. Note that the prediction error in the final vehicle velocity can be neglected, and therefore the constraint on v_{rel} is not altered.

5.2. *RG with vehicle prediction*

Results with the combined RG, i.e. the robustified setpoint optimisation and the vehicle prediction, are generated with identical setting as previously, so $T = 0.1$ ms, $T_o = 10$ ms, $T_e = 200$ ms, $L_1 = -0.03$ m, $L_2 = 0.25$ m, $S_1 = -1$m/s, $S_2 = 0$ m/s, $m = 9$, $\beta_1 = \beta_2 = 1$, and $\beta_3 = 10$. Figure 8 shows the results of the combined robust RG for the same EuroNCAP frontal impact pulse as in Figure 6. The RG starts at $t = 2T_o = 20$ ms, because the error in the vehicle prediction is too large at $t = T_o$, as can be observed in Figure 7(b), and an appropriate setpoint cannot be determined. For $t < 20$ ms, the setpoint is set to equal the measured crash pulse, as this will keep the occupant restrained to the seat.

Obviously, the calculation times were higher than for the case in which it was assumed that full *a priori* knowledge of the crash is available, see Figure 6. The prediction step takes no

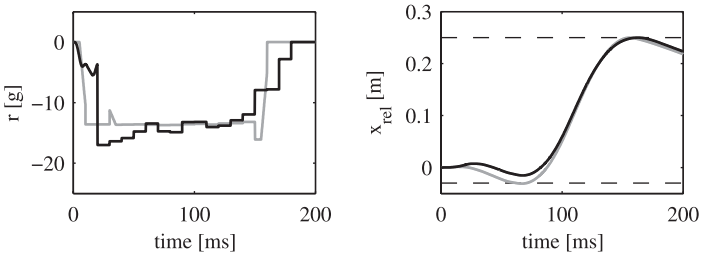

Figure 8. Left: The optimal setpoint r for the chest acceleration with (grey) and without (black) prior knowledge of the crash pulse. Right: Corresponding relative chest displacement.

more than 2 ms on average, as it consists merely of some matrix multiplications. However, the constraints are tighter in the robustified version (22), and the LP solver needs more time, viz. 10 ms compared with 6 ms, to find the optimal solution. In standard high-level computing language (Matlab), solutions were hence found within 12 ms. When the algorithms are efficiently rewritten in a middle-level language, for example C++, it is more than reasonable to assume that the solutions can be found within $T_o = 10$ ms, thereby meeting the real-time requirements.

The results show that the calculated setpoint, based on the vehicle prediction, is desirably close to the optimal setpoint, obtained with full *a priori* crash information as in Section 3.4. This implies that *without* knowledge of the crash, close to optimal behaviour can be predicted in terms of the injury parameter $A_{\max}$ for the considered impact pulse.

5.3. *Results with a MADYMO primal controlled loop*

In this section, the RG is applied to a more realistic, primal controlled system. This system has reasonably well tracking properties, i.e. $y = a_{\text{chest}} \approx r$, instead of $y = r$. So in other words, Assumption 2.4 is somewhat relaxed.

The numerical, primal compensated system consists of a 50 percentile Hybrid III dummy from the MADYMO database [47]. The airbag system is disabled, and the conventional belt load limiter is replaced by a belt force actuator. The occupant is seated in an interior compartment model, representing a small family car. The controller consists of an integrator with appropriate gain and is designed such that the chest acceleration tracks the desired trajectory r. For more details on this model, the interested reader is referred to [15,28].

Results for the controlled chest acceleration using the setpoint from the RG are shown in Figure 9 together with the required belt force. Results are compared with responses from an identical occupant model with a conventional belt restraint system, i.e. a 4 kN load limiter. It can be seen that the $A_{\max}$ criterion has reduced by approximately 45%. Although not shown in this figure, the peak chest deflection, $D_{\max}$, is also lowered, in spite of the higher belt forces. This can be understood from the fact that the peak chest acceleration has been reduced, which indicates that the forces acting on the thorax are lower. To emphasise the relevance of these results, note that the only inputs to the RG algorithm are the initial vehicle velocity v_o, and the measured *current* vehicle and chest acceleration, a_{veh} and a_{chest}, respectively. However, it should be mentioned that this injury reduction is achieved with an ideal belt actuator and perfect sensors, which is, of course, in practice not realisable. Still, it is believed that it is possible to harvest a major part of the $A_{\max}$-reduction, since the primal controller can be accommodated to the near ideal actuator, and to the filtering properties of the estimator.

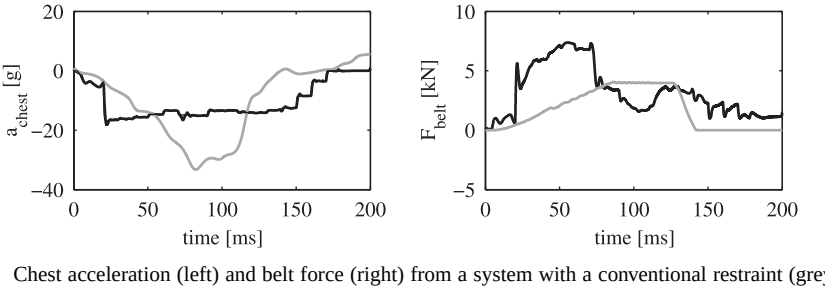

Figure 9. Chest acceleration (left) and belt force (right) from a system with a conventional restraint (grey) and a primal controlled system with the RG as proposed in this paper (black).

6. Discussion and future work

In this paper, a novel control strategy for real-time control of adaptive belt restraint systems is proposed. The control method consists of a combination of a primal controlled loop, which achieves good tracking properties, and a modified RG. The RG finds an optimal setpoint for the chest acceleration, while satisfying constraints and without having *a priori* knowledge of the upcoming crash. The RG includes a vehicle motion estimation procedure to obtain goods estimates of the vehicle position during the crash. The complete RG is robustified with respect to these uncertain prediction errors.

Moreover, the whole design procedure is generic in nature. For instance, it is straightforward to include multiple IC in the design process. Also, different primal controllers and plant dynamics can be accounted for. This flexibility enables the inclusion of various future improvements, such as novel actuators and sensor technologies.

In summary, the RG control strategy is believed to be an important step towards real-time implementation of controlled passive safety systems. It reduces the IC considerably (for example, $A_{\max}$ for a EuroNCAP pulse with 45% with respect to conventional to conventional restraint systems) while still meeting the real-time computational requirements.

Interestingly, the performance of the overall RG scheme can even be improved when accurate pre-crash information systems, for example on closing speed or impact angle, become available in the near future. The reason is that the vehicle motion prediction can be significantly improved. This could potentially lead to a further reduction of injury risk even beyond the achieved reductions, which were already significant.

Acknowledgements

This work is supported by TNO Automotive, Helmond in the Netherlands, and the authors would like to thank them for their support.

Note

1. The code was written in Matlab M-code, and simulations were performed on a workstation with a CPU that runs at 1.4 GHz.

References

[1] U. Seiffert and L. Wech, *Occupant protection*, in: *Automotive Safety Handbook*, 2nd ed. Society of Automotive Engineers (SAE), Warrendale, USA, 2007, pp. 151–182.
[2] National Highway Traffic Safety Administration (NHTSA), *Federal Motor Vehicle Safety Standard (FMVSS)* Part 571, Crashworthiness, US Department of Transportation, Washington, DC, USA, 1998.
[3] Office of Crashworthiness Standards, *Laboratory Test Procedure for US New Car Assessment Programme (USNCAP)*, Frontal impact testing, National Highway Traffic Safety Administration (NHTSA) and US Department of Transportation, Washington, DC, USA, 1996.
[4] IIHS, *Frontal Offset Crashworthiness Evaluation: Offset Barrier Crash Test Protocol* version XIII, Insurance Institute for Highway Safety (IIHS), Arlington, VA, USA, 2008.
[5] EuroNCAP, *Frontal Impact Testing Protocol* v4.2, European New Car Assessment Protocol (EuroNCAP), Brussels, Belgium, 2008.
[6] H.J. Miller, *Injury reduction with smart restraint systems*, in Proceedings of the 39th Annual Meeting of the Association for the Advancement of Automotive Medicine (AAAM), October 16–18, AAAM, Chicago, IL, USA, 1995, pp. 527–541.
[7] R.W. Kent, D.V. Balandin, N.N. Bolotnik, W.D. Pilkey, and S.V. Purtsezov, *Optimal control of restraint forces in an automobile impact*, J. Dyn. Syst. Meas. Control Trans. ASM 129 (2007), pp. 415–424.
[8] A.R. Bernat, *'Smart' Safety belts for injury reduction*, in Proceedings of the 39th Annual Association for the Advancement of Automotive Medicine (AAAM), 16–18 October, AAAM, Chicago, IL, USA, 1995, pp. 567–576.

[9] M. Mackay, *Smart seat belts – Some population considerations applied to intelligent restraint systems*, in Proceedings of the SAE International Congress and Exposition, no. 940531, in SAE Tech. Papers, 28 February – 3 March, Society of Automotive Engineers (SAE), Detroit, MI, USA, 1994, pp. 13–22.
[10] H.J. Miller, *Restraint force optimization for a smart restraint system*, in Proceedings of the SAE International Congress and Exposition, no. 960662, In SAE Tech. Papers, 26–29 February, Society of Automotive Engineers (SAE), Detroit, MI, USA, 1996, pp. 79–84.
[11] M.F. Murad, E. Burley, and B. Blackburn, *Integrated CAE modeling of intelligent restraint systems*, in Proceedings of the SAE 2000 World Congress, no. 2000-01-0606, in SAE Tech. Papers, 6–9 March, Society of Automotive Engineers (SAE), Detroit, MI, USA, 2000.
[12] J.A. Musiol, L.M. Norgan-Curtiss, and M.D. Wilkins, *Control and application of intelligent restraint systems*, in Proceedings of the SAE International Congress and Exposition, no. 971052, in, SAE Tech. Papers, 24–27 February, Society of Automotive Engineers (SAE), Detroit, MI, USA, 1997, pp. 1–8.
[13] H. Johannessen, *Why intelligent automotive occupant restraint systems?*, in Proceedings of the 39th Annual Association for the Advancement of Automotive Medicine (AAAM), 16–18 October, AAAM, Chicago, IL, USA, 1995, pp. 519–525.
[14] P. Holding, B. Chinn, and J. Happian-Smith, *An evaluation of the benefits of active restraint systems in frontal impacts through computer modelling and dynamic testing*, in Proceedings of the 17th International Technical Conference on the Enhanced Safety of Vehicles (ESV), 328, 4–7 June, NHTSA, Amsterdam, The Netherlands, 2001, pp. 1–9.
[15] R.J. Hesseling, *Active restraint systems; feedback control of occupant motion*, Ph.D. thesis, Technische Universiteit Eindhoven, The Netherlands, 2004.
[16] J. Cooper, P. Lemmen, and C. van Schie, *Effectiveness of real time control for active restraint systems in frontal crashes*, in Proceedings of Airbag 2004, 29 November – 1 December, Fraunhofer-Institut für Chemische Technologie (ICT), Karlsruhe, Germany, 2004, pp. 1–7.
[17] M.S. Habib, *Active control of vehicle occupant's motion in front- and rearend collisions*, in Proceedings of the Automotive and Transportation Technology Congress and Exhibition, no. 2001-01-3430, in SAE Tech. Papers, 1–3 October, Society of Automotive Engineers (SAE), Barcelona, Spain, 2001, pp. 1–9.
[18] H. Adomeit, E. Wils, and A. Heym, *Adaptive airbag-belt-restraints – an analysis of biomechanical benefits*, in Proceedings of the SAE International Congress and Exposition, no. 970776, in, SAE Tech. Papers, 24–27 February, Society of Automotive Engineers (SAE), Detroit, MI, USA, 1997, pp. 163–177.
[19] H. Shin, T. Yeo, and W. Ha, *The numerical study for the adaptive restraint system*, in Proceedings of the SAE 2007 World Congress, no. 2007-01-1500, in, SAE Tech. Papers, 16–19 April, Society of Automotive Engineers (SAE), Detroit, MI, USA, 2007.
[20] T.J. Paulitz, D.M. Blackketter, and K.K. Rink, *Fully-adaptive seatbelts for frontal collisions*, in Proceedings of the 19th International Technical Conference on the Enhanced Safety of Vehicles (ESV), 127, 6–9 June, NHTSA, Washington, DC, USA, 2005, pp. 1–12.
[21] G. Clute, *Potentials of adaptive load limitation presentation and system validation of the adaptive load limiter*, in Proceedings of the 17th International Technical Conference on the Enhanced Safety of Vehicles (ESV), 4–7 June, NHTSA, Amsterdam, The Netherlands, 2001, pp. 113–134.
[22] H.J. Miller, *Occupant performance with constant force restraint systems*, in Proceedings of the SAE International Congress and Exposition, no. 960502, in SAE Tech. Papers, 26–29 February, Society of Automotive Engineers (SAE), Detroit, MI, USA, 1996, pp. 17–27.
[23] T.J. Paulitz, D.M. Blackketter, and K.K. Rink, *Constant force restraints for frontal collisions*, Proc. Inst. Mech. Eng. Part D: J. Automobile Eng. 220 (2006), pp. 1177–1189.
[24] H.J. Mertz, J.E. Williamson, and D.A. van der Lugt, *The effect of limiting shoulder belt load with airbag restraint*, in Proceedings of the SAE International Congress and Exposition, no. 950886, in SAE Tech. Papers, 27 February – 2 March, Society of Automotive Engineers (SAE), Detroit, MI, USA, 1995, pp. 185–192.
[25] T. Iyota and T. Ishikawa, *The effect of occupant protection by controlling airbag and seatbelt*, in Proceedings of the 18th International Technical Conference on the Enhanced Safety of Vehicles (ESV), no. 198, 19–22 May, NHTSA, Nagoya, Japan, 2003, pp. 1–10.
[26] J.R. Crandall, Z. Cheng, and W.D. Pilkey, *Limiting performance of seat belt systems for the prevention of thoracic injuries*, J. Automobile Eng. 214 (2000), pp. 127–139.
[27] R.J. Hesseling, M. Steinbuch, F.E. Veldpaus, and T. Klisch, *Feedback control of occupant motion during a crash*, Int. J. Crashworthiness 11 (2006), pp. 81–96.
[28] E.P. van der Laan, F.E. Veldpaus, A.G. de Jager, and M. Steinbuch, *Control oriented modeling of occupants in frontal impacts*, Int. J. Crashworthiness, (2009), in press.
[29] M. Kleinberger, E. Sun, R.H. Eppinger, S. Kuppa, and R. Saul, *Development of improved injury criteria for the assessment of advanced automotive restraint systems*, Report, National Highway Traffic Safety Administration (NHTSA), 1998.
[30] A.I. King, *Fundamentals of impact biomechanics: Part 1 - biomechanics of the head, neck, and thorax*, Ann. Rev. Biomed. Eng. 2 (2000), pp. 55–81.
[31] J.M. Cavanaugh, *The biomechanics of thoracic trauma*, in *Accidental Injury – Biomechanics and Prevention*, 1st ed. Springer-Verlag, New York, 1993, pp. 362–428.
[32] Siemens VDO Inc., *Wedgetronic Seatbelt*, Product sheet, 2008; Available at http://www.siemensvdo.com.
[33] C.E. Garcia, D.M. Prett, and M. Morari, *Model predictive control: Theory and practice – a survey*, Automatica 25 (1989), pp. 335–348.

[34] M. Morari and J.H. Lee, *Model predictive control: Past, present and future*, Comput. Chem. Eng. 23 (1999), pp. 667–682.
[35] J.M. Maciejowski, *Predictive Control with Constraints*, Prentice Hall, Harlow, UK, 2001.
[36] D.Q. Mayne, J.B. Rawlings, C.V. Rao, and P.O.M. Scokaert, *Constrained model predictive control: Stability and optimality*, Automatica 36 (2000), pp. 789–814.
[37] A. Bemporad, W.P.M.H. Heemels, and B. de Schutter, *On hybrid systems and closed-loop MPC systems*, IEEE Trans. Automat. Contr. 47 (2002), pp. 863–869.
[38] A. Bemporad, M. Morari, V. Dua, and E.N. Pistikopoulos, *The explicit linear quadratic regulator for constrained systems*, Automatica 38 (2002), pp. 3–20.
[39] P. Tøndel, T.A. Johansen, and A. Bemporad, *An algorithm for multi-parametric quadratic programming and explicit MPC solutions*, Automatica 39 (2003), pp. 489–497.
[40] E.G. Gilbert and I. Kolmanovsky, *Nonlinear tracking control in the presence of state and control constraints: A generalized reference governor*, Automatica 38 (2002), pp. 2063–2073.
[41] E.G. Gilbert and I. Kolmanovsky, *Fast reference governors for systems with state and control constraints and disturbance inputs*, Internat. J. Robust Nonlinear Control 9 (1999), pp. 1117–1141.
[42] A. Bemporad, *Reference governors for constrained linear system*, IEEE Trans. Automat. Contr. 43 (1998), pp. 415–419.
[43] A. Bemporad, A. Casavola, and E. Mosca, *Nonlinear control of constrainted linear systems via predictive reference management*, IEEE Trans. Automat. Contr. 42 (1997), pp. 340–349.
[44] E.P. van der Laan, F.E. Veldpaus, and M. Steinbuch, *State estimator design for real-time controlled restraint systems*, in Proceedings of the American Control Conference (ACC), 11–13 July, IEEE, New York City, USA, 2007, pp. 242–247.
[45] S.P. Boyd and L. Vandenberghe, *Convex Optimization*, Vol. 1, Cambridge University Press, UK, 2004.
[46] R. Cagienard, P. Grieder, E.C. Kerrigan, and M. Morari, *Move blocking strategies in receding horizon control*, J. Process Control 17 (2007), pp. 563–570.
[47] TNO MADYMO B.V., *MADYMO Manual*, Version 6.3, TNO Road-Vehicles Research Institute, Delft, The Netherlands, 2005.